energies

MDPI

Article

Determining the Burning Rate of Fine-Grained Propellants in Closed Vessel Tests

Radosław Trębiński *, Zbigniew Leciejewski and Zbigniew Surma

Faculty of Mechatronics, Armament and Aerospace, Institute of Armament Technology, Military University of Technology, 2 Gen. S. Kaliskiego Street, 00-908 Warsaw, Poland; zbigniew.leciejewski@wat.edu.pl (Z.L.); zbigniew.surma@wat.edu.pl (Z.S.)

* Correspondence: radoslaw.trebinski@wat.edu.pl

Abstract: This paper presents the method of determining the burning rate of fine-grained propellants based on the results of closed vessel tests. It is shown that in the case of fine-grained propellants, the standard methods of determining the burning rate fail. There are two reasons for this: imperfections of the grain shapes and the prolonged process of ignition due to a more developed surface than that of coarse grains at the same mass of the propellant. The value of the exponent in the burning law is estimated by the use of the so-called experimental form–function. The upper and lower limits of the value of the coefficient in the burning law are estimated. The accuracy of the proposed method is analyzed. Its validity is assessed by comparing the results of closed vessel tests analysis with accessible literature data.

Keywords: closed vessel test; burning rate; form–function; fine-grained propellants

Citation: Trębiński, R.; Leciejewski, Z.; Surma, Z. Determining the Burning Rate of Fine-Grained Propellants in Closed Vessel Tests. *Energies* **2022**, *15*, 2680. https://doi.org/10.3390/en15072680

Academic Editors: Michael Liberman and Rob J. M. Bastiaans

Received: 1 March 2022
Accepted: 4 April 2022
Published: 6 April 2022

1. Introduction

The dependence of the burning rate of propellants on the pressure and initial temperature is one of their most important characteristics from the point of view of their applications in gun systems. The standard methods of experimental determination of the burning rate are described in monographs [1–4], in standardization documents [5], and in descriptions of computer codes [6–9]. Nonstandard approaches can be found in several publications [10,11]. Theoretical methods have also been developed, starting from the early work of Zeldovich [12]. However, as stated in a review paper by [13], the theoretical methods cannot be treated as predictive tools for determining the burning rate values. Therefore, ballisticians must rely on experimental methods. There are two such methods: strand burner tests and closed vessel tests (CVT). In the first method, the propellant should have the form of a strand. In CVT, the propellant can be in its usual granular form.

The methods based on CVT, as described in the literature, give rational burning rate values in the case of coarse-grained propellants, which have regular geometric forms. However, they fail in the case of the fine-grained propellants used in small arms. The forms of grains of these propellants show deviations from perfect geometry. Moreover, their process of ignition in CVT is prolonged. A considerable part of the propellant charge must be burned before the whole charge is ignited. This can be explained in the following way: In order to ignite a propellant grain, a thin layer of the propellant must be preheated. The volume of this layer can be roughly assessed as a product of the grain surface area and the thickness of the preheated layer d. The value of d is roughly the same for fine and coarse grains. Therefore, the volume of the preheated propellant of a given mass is larger for fine grains, because the global surface area is larger. This means that a larger value of the energy of the igniter is necessary to ignite a propellant charge composed of fine grains. As shown in [14,15], increasing the mass of the igniter is not a solution, because it prolongs the time of parallel burning of the igniter and the propellant. Moreover, in ammunition, the correlation between the igniter mass and propellant mass is even lower than that applied in CVT.

During the development of new models of small arms undertaken in our university, a problem was encountered in the acquisition of reliable data for interior ballistics modeling. The problem consists of determining the burning rate of fine-grained propellants used in the ammunition for the small arms. The methods described in the literature do not give reliable results. Therefore, a method for determining the burning rate of fine-grained propellants needs to be invented that takes into account the prolonged process of their ignition in CVT. In this paper, such a method is proposed. The method is based on some ideas proposed in [16,17]. This paper presents the final stage of the evolution of that method.

In the description of the method, it is first demonstrated that the standard method of determining the values of the exponent and the coefficient in the burning law gives rational results in the case of coarse-grained propellants and fails in the case of fine-grained propellants. Then, the method of determining the value of the exponent in the burning law is presented. The accuracy of the method is analyzed on the basis of CVT results. Then, two alternative methods of determining the value of the coefficient in the burning law are described. On the basis of the detailed analysis, it is concluded that these methods provide an assessment of the lower and upper limits of the value of the coefficient. The methods of determining the values of the exponent and the coefficient in the burning law are validated on the basis of a comparison of their results with accessible literature data.

2. Method

In closed vessel tests, a charge of the given propellant mass m_p was ignited by combustion of a given mass of the igniter (black powder). Combustion of the igniter produced ignition pressure p_{ign}. The pressure–time courses $p(t)$ produced by the combustion of the tested propellant were measured. A collection of $p(t)$ for several values of the loading density Δ formed the output of the CVT. Based on the maximum values of pressure, coefficients of the equation of state of the propellant gases were calculated. For the most popular Noble–Abel equation, these coefficients are propellant force f and co-volume η. The burning rate r can be determined by using the following formulae (based on [5]):

$$r = \frac{de_{gb}}{dt} = \frac{de_{gb}}{dz}\frac{dz}{dp}\frac{dp}{dt} \tag{1}$$

$$\frac{de_{gb}}{dz} = \frac{V_{g0}}{S_{g0}\phi(z)} \tag{2}$$

$$z = \frac{b_1 p_s}{f + b_2 p_s}, \quad p_s = p - p_{ign}, \quad b_1 = \frac{1}{\Delta} - \frac{1}{\rho}, \quad b_2 = \eta - \frac{1}{\rho} \tag{3}$$

$$\frac{dz}{dp} = \frac{b_1 f}{(f + b_2 p_s)^2} \tag{4}$$

where e_{gb} is the thickness of the burned layer of the propellant, z is the relative burned volume of the propellant, V_{g0} is the initial volume of grain, S_{g0} is the initial surface area of grain, $\phi(z)$ is form–function ratio (ratio of the actual surface area of a burning grain to its initial value), and ρ is the propellant grain density.

The function $r(p)$ obtained in the tabular form is approximated by an analytical expression. Vielle's law is the most popular approximation, which is

$$r = \beta(p/p_0)^{\alpha}, \quad p_0 = 0.1\,\text{MPa} \tag{5}$$

Equation (5) differs from the widely used convention ([1–4]). In the authors' opinion, however, this form is convenient because coefficient β is expressed in the same units as the burning rate r. From Equation (5), the following relation follows:

$$\log_{10} r = \log_{10} \beta + \alpha \log_{10}(p/p_0) \tag{6}$$

Approximating this relation by the linear function, the values of α and β can be calculated. Figure 1 presents this approximation for the double-based LO5460 (JA-2) propellant produced by Nitrochemie AG. Plots for the single-based NC1214 Bofors propellant are shown in Figure 2 for comparison. They have no parts that can be approximated by a straight line. The difference in the plots for the two propellants results from the geometric characteristics of their grains. As shown in Figures 3 and 4, LO5460 has very regular grains, while the NC1214 grain shapes are far from perfect. However, this is not the only reason for the observed difference in the character of the $\log_{10} r(p)$ plots.

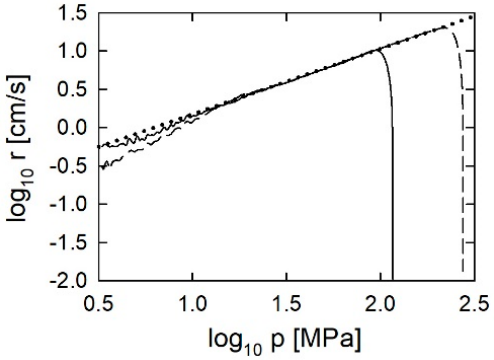

Figure 1. Log_log plots of $r(p)$ for LO5460; Δ = 100 kg/m^3 (solid line), 200 kg/m^3 (dashed line).

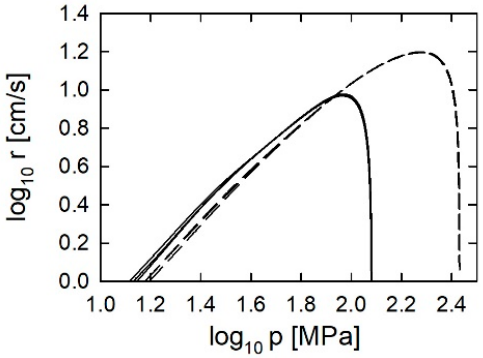

Figure 2. Log_log plots of $r(p)$ for NC1214 Δ = 100 kg/m^3 (solid line), 200 kg/m^3 (dashed line).

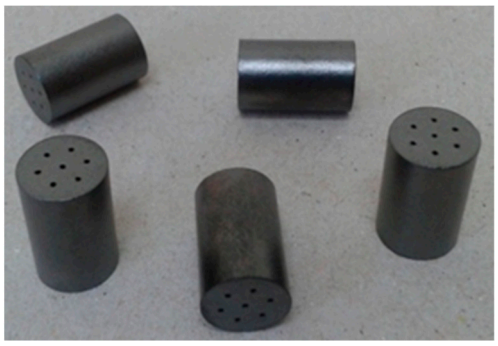

Figure 3. Image of LO5460 grains.

Figure 4. Image of NC1214 grains.

The global surface of the propellant charge of a given mass scales with S_{g0}/V_{g0}. The values of this parameter for LO5460 and NC1214 are given in Table 1, together with values referring to other propellants analyzed in this paper. The value of S_{g0}/V_{g0} = 1.5 mm^{-1} can be proposed as indicative of the classification of the propellants from the point of view of their grain sizes. If the S_{g0}/V_{g0} value is higher than this amount, the propellant is classified as fine-grained.

Table 1. Values of the ratio of the initial grain surface to the initial volume for propellants referred to in the paper.

Propellant	S_{g0}/V_{g0} [1/mm]
(DB) LO5460	0.813
(SB) NC1214	3.850
(SB) 5/7NA	2.977
(SB) 12/7	1.190

DB double-base, SB single-base.

The S_{g0}/V_{g0} value is 4.7 times higher for NC1214 than for LO5460. This means that roughly 4.7 times more energy is necessary to ignite NC1214 grains. The energy delivered by the igniter is not sufficient. A considerable part of the propellant charge must be burned so as to deliver enough energy to ignite the whole charge. This means that the values of z for individual grains differ. Therefore, the value of z in Equations (1)–(4) does not refer to individual grains but is the relative burned mass of the whole charge. This means that Equation (2) cannot be used, because it is based on the assumption that all the grains are identical and that they are ignited at the same time. The combustion of individual grains should thus be considered. The rate of the mass change in a grain numbered i can be expressed as

$$dm_{gi}/dt = \rho S_{gi} r_i \tag{7}$$

When summing up n_g grains included in the propellant charge of the mass m_p, we obtain

$$dm_p/dt = \rho \sum_{i=1}^{n_g} S_{gi}\, r_i \tag{8}$$

Assuming that all grains burn at the same rate r, we can represent (8) in the following form:

$$dm_p/dt = \rho r \sum_{i=1}^{n_g} S_{gi} \tag{9}$$

Dividing both sides of Equation (9) by the initial mass of the propellant, we obtain

$$dz/dt = \left(\rho r \sum_{i=1}^{n_g} S_{gi}\right) / \left(n_g \rho\, V_{g0}\right) \tag{10}$$

Let us represent Equation (10) in the following form:

$$dz/dt = S_{g0}/V_{g0}\, r \left[\sum_{i=1}^{n_g} \left(S_{gi0}/S_{g0}\right)\left(S_{gi}/S_{gi0}\right)\right] / n_g \tag{11}$$

The ratio S_{g0}/V_{g0} has a sense of the mean ratio for all grains in the charge. It is equal to the ratio of the total surface area to the total volume of all grains in the charge. The relative burning surface $\phi_i = S_{gi}/S_{gi0}$ is a function of the relative burnt mass of propellant grain z_i and is determined by the form of grain i. We define the function

$$\phi_{ex}(z) = \sum_{i=1}^{n_g} \left(S_{gi0}/S_{g0}\right)\phi_i(z_i)/n_g \tag{12}$$

when all grains are identical, and they are ignited at the same time, $z_i = z$ and $\phi_{ex}(z)$ is identical to $\phi(z)$. However, when grains are ignited gradually, $\phi_{ex}(z)$ is an average form–function. It depends not just on the shapes and sizes of the grains but on the details of the ignition process as well. Therefore, we call it an "experimental form–function". Using Equations (5), (11) and (12) we have

$$dz/dt = \theta\, \phi_{ex}(z)(p/p_0)^{\alpha}, \quad \theta = S_{g0}/V_{g0}\, \beta \tag{13}$$

We introduce the function $G(z)$ as follows:

$$G(z) = \theta\, \phi_{ex}(z) \tag{14}$$

Therefore, we can represent Equation (13) in the following form:

$$dz/dt = G(z)(p/p_0)^{\alpha} \tag{15}$$

The values of dz/dt as a function of z and p can be calculated using Equations (3) and (4) and the relation

$$dz/dt = (dz/dp)(dp/dt) \tag{16}$$

The value of the exponent α can be determined on the basis of the following relation:

$$\log_{10}(dz/dt) = \log_{10}[G(z)] + \alpha\, \log_{10}(p/p_0) \tag{17}$$

By calculating dz/dt values for several values of the loading density and the same value of z, we can treat Equation (17) as a linear correlation between $\log_{10}(dz/dt)$ values and $\log_{10}(p/p_0)$ values. The slope determines the value of α; thus, the α values for z = 0.3, 0.4, 0.5, 0.6, and 0.7 are determined, and then the average value is calculated. Knowing this value, we can calculate the values of $G(z)$.

To determine the burning rate, the value of coefficient β is necessary. It can be determined only in an approximate way by relating function $G(z)$ to the theoretical form–function $\phi(z)$. Various methods of determining the β value were proposed in [16,17]. In this study, we propose two other methods, which are—in our opinion—better justified. The lower limit of the β value (β_1) is determined on the basis of the integration of Equation (5) in a chosen z range [z_1,z_2] as follows:

$$e_{gb}(z_2) - e_{gb}(z_1) = \beta_1 \int_{t(z_1)}^{t(z_2)} \xi^{\alpha} dt, \quad \xi(t) = p(t)/p_0 \tag{18}$$

Changing the integral variable, we have

$$e_{gb}(z_2) - e_{gb}(z_1) = \beta_1 \int_{z_1}^{z_2} \xi^{\alpha} \frac{dt}{dz} dz \tag{19}$$

Making use of Equation (15), we can transform Equation (19) to

$$e_{gb}(z_2) - e_{gb}(z_1) = \beta_1 \int_{z_1}^{z_2} \frac{dz}{G(z)} \tag{20}$$

Therefore, the β value can be calculated as

$$\beta_1 = \frac{e_{gb}(z_2) - e_{gb}(z_1)}{\int_{z_1}^{z_2} G^{-1}(z) dz} \tag{21}$$

The quantity $e_{gb}(z)$ has a sense of the mean value of the thickness of the burned layer. Its approximate value is calculated based on the theoretical form–function. After calculating the β_1 value, the θ_1 value can be calculated as follows:

$$\theta_1 = S_{g0}/V_{g0}\beta_1 \tag{22}$$

The upper limit of the β value (β_2) is determined based on the assumption that the relative burning area does not exceed the theoretical value

$$\theta_2 = \max_{z \in [z_0, 1]} [G(z)/\phi(z)] \tag{23}$$

The lower limit of the z range z_0 is chosen in such a way that the part of the $G(z)$ curve that corresponds to the initial transient process, when the tested propellant burns parallel with the igniter, is eliminated. As shown in [15], burning of the tested propellant begins before attaining the ignition pressure, and burning of the igniter ends at pressure values higher than the ignition pressure. At low values of pressure, the igniter burns considerably faster than the tested propellant. Therefore, the dp/dt values are high, and consequently, the $G(z)$ values are larger than in the case when the tested propellant burns alone.

After determining the θ_2 value, the β_2 value can be calculated as follows:

$$\beta_2 = V_{g0}/S_{g0}\theta_2 \tag{24}$$

3. Results and Discussion

For the analysis of the described method, the results of closed vessel tests for the single-base seven-perforated 5/7NA propellant produced by Pionki SA (Poland) were chosen. Details of the experiments were presented in [16]. The propellant has an S_{g0}/V_{g0} value 3.7 times larger than LO5460, so it can be classified as a fine-grained propellant. Closed vessel tests were performed for seven values of the loading density Δ: 100, 125, 150, 175, 200, 225, and 250 kg/m^3. For each value of Δ, seven tests were performed. Thus, very useful results for statistical analyses were obtained.

Figure 5 presents the calculated $\log_{10}(dz/dt)$ values as a function of the $\log_{10} p$ and z values. Dashed lines represent the linear approximation. Points along a given line correspond to different values of Δ. The slopes of the approximation lines are different.

Therefore, different values of α correspond to them. These are shown in Figure 6 for pressure ranges corresponding to the ranges of the plots in Figure 5. The scatter of α values is a result of differences in $G(z)$ functions for various loading density values. Their plots are shown in Figure 7. The initial ascending parts of the plots correspond to the ignition process. It can be seen that, for low values of Δ, considerable parts of the propellant charges are burned before the complete ignition. For the range of z [0.3,0.7], the differences between the $G(z)$ plots are relatively low. That is why this range was chosen for determining the value of α. Nevertheless, Equation (17) can be treated only as approximate, and therefore, the α values calculated on its basis are also approximations. The accuracy of the value of α can be improved by calculating it as an average of the values calculated for z = 0.3, 0.4, 0.5, 0.6, and 0.7. For the plot shown in Figure 6, it is 0.847. It is interesting that this value is very close to the value of 0.85, which is typical for double-base propellants in the range of high-pressure values [18].

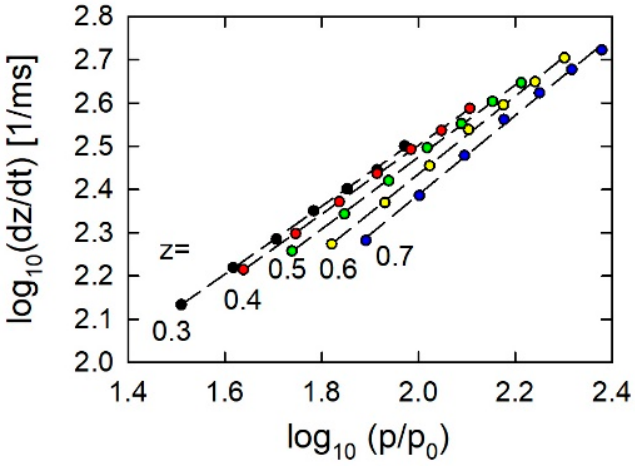

Figure 5. Plots of $\log_{10}(dz/dt)$ versus $\log_{10}p$.

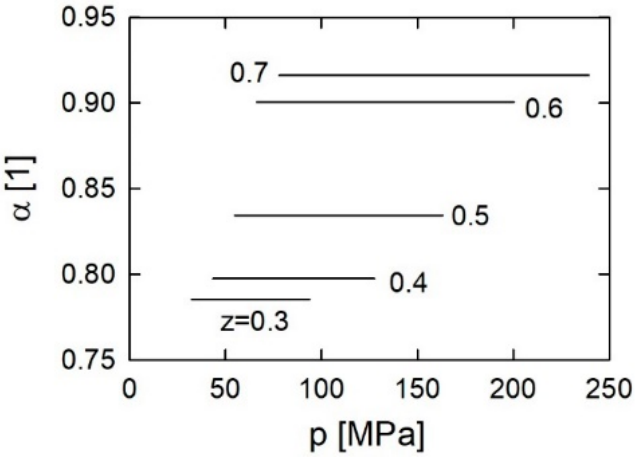

Figure 6. Values of the exponent α for chosen z values.

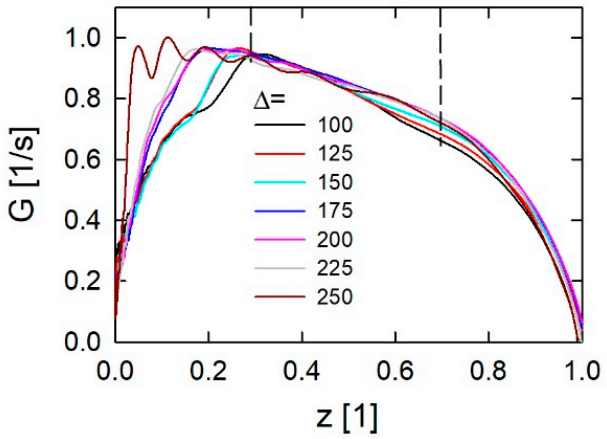

Figure 7. Plots of $G(z)$ functions.

The plots shown in Figures 5–7 were determined using the results of only one of the seven tests for a given Δ. After performing the analysis for each of the seven tests, a set of α values was obtained. The mean value was equal to 0.837 ± 0.020. The scatter of α values, assessed for a 0.95 confidence level, formed 2.5% of the mean α value. Therefore, we can assess that the repeatability of the method of determining the α values is very good. This suggests that a limited number of tests can be performed for determining the value of α. In order to check this, the results of two tests for $\Delta = 100$ kg/m^3 and two tests for $\Delta = 200$ kg/m^3 were chosen randomly. Therefore, the results of only four tests were used for determining the α value. The obtained value of 0.843 was within the assessed scatter range of α values, determined on the basis of the results of 49 tests.

After determining the α value, function $G(z)$ can be determined based on Equation (15). In the next step, the value of β can be determined using Equation (21) or Equation (24). In Equation (21), the z_1 and z_2 values were set as 0.3 and 0.7, respectively. Figure 8 presents the values of the coefficient θ calculated by Equation (22) (θ_1) and Equation (23) (θ_2). It demonstrates the level of uncertainty of the θ value and, resulting from this, the uncertainty of the β value. The two proposed methods provide only the lower and upper limits. Moreover, for a given method, different values were determined for various loading density values.

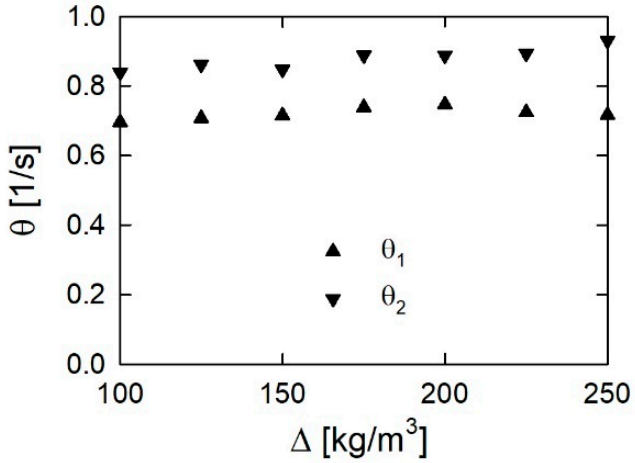

Figure 8. Values of coefficient θ, determined by two methods.

Making use of Equation (14), the experimental form–function was determined. The average values of θ_1 and θ_2 were used. Figures 9 and 10 present experimental form–function plots calculated using θ_1 and θ_2, respectively. The plots were compared with the plots of the theoretical form–function. The differences between the experimental and

theoretical form–function plots are pronounced. This demonstrates why the method of determining the burning rate described in STANAG4115 [5] cannot be used in the case of fine-grained propellants.

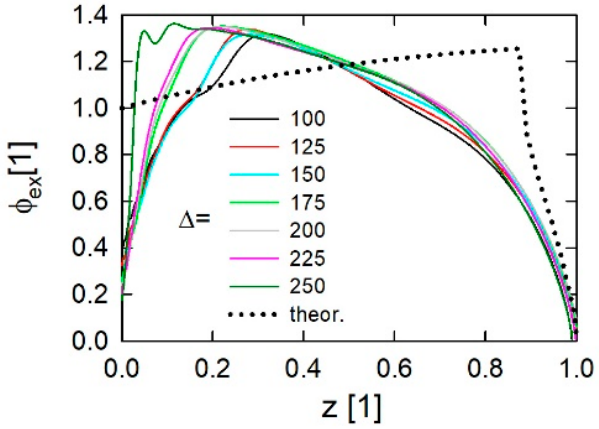

Figure 9. Plots of the experimental form–functions calculated using the mean θ_1 value.

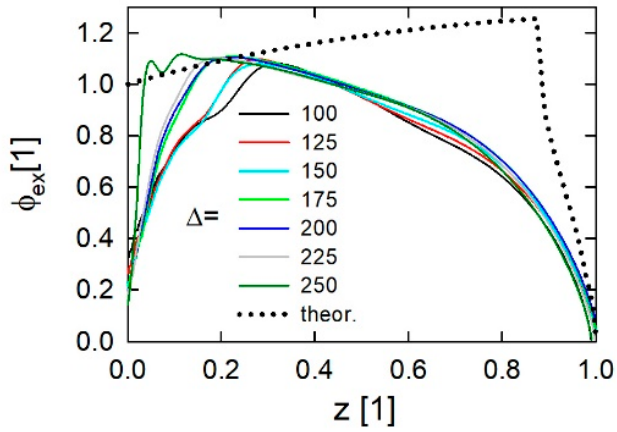

Figure 10. Plots of the experimental form–functions calculated using the mean θ_2 value.

The use of the θ_1 value results in $\phi_{ex}(z)$ values exceeding the $\phi(z)$ values in a range of z values (Figure 9). This raises the question, can the relative burning surface area exceed its theoretical value? It is possible from a purely mathematical point of view. The mean value of the nonlinear function $\phi(z)$ differs from its value for the mean z value. However, the relation between $\phi_{ex}(z)$ and $\phi(z)$ plots in Figure 9 can also be the result of the limited accuracy of calculating the S_{g0}/V_{g0} value. We calculated it by measuring the sizes of a limited number of grains, averaging the results of the measurements, and assuming the ideal shape of propellants grains. Due to imperfections of grain shapes, the real value of S_{g0}/V_{g0} can be larger than the value determined in the way described above. A larger value of S_{g0}/V_{g0} means that the value of θ_1 can be larger, and $\phi_{ex}(z)$ can be lower.

There is another reason that causes the θ_1 value to diminish. The prolonged ignition causes the time of combustion of the charge to be longer than in the case of the immediate ignition of the whole charge. The same can be said referring to the time span $t(z_2)$–$t(z_1)$ in the integral in Equation (18). This means that the value of the integral is higher than that in the case of the immediate ignition. This causes the β_1 value, and consequently the θ_1 value, to diminish.

There are some physical reasons that may cause the $\phi_{ex}(z)$ values to exceed the $\phi(z)$ values. Grains that have delayed ignition undergo relatively long heating before they ignite. Although the intensity of the heat flux is too low to cause fast ignition, it increases the temperature inside the grain. After ignition, the flame propagates into the heated material,

which causes the burning rate to be higher. Apparently, this is equivalent to an increase in the burning surface area. In the case of fine-grained propellants, the thickness of the heated layer may form a considerable part of the web. Therefore, the effects of the heating prior to the ignition may influence the experimental form–function.

Another physical effect is the crushing of some grains. After ignition, the pressure field around the grain is approximately isostatic. However, before ignition, the intergranular stresses may exceed the strength of the propellant, causing large deformation and crushing. As shown in [19], cracks inside propellant grains occur under dynamic deformation. During crushing, new surfaces are formed. After their ignition, the total burning surface may exceed the initial surface. Fragments of grains caused by crushing burn with a fast-decreasing surface area (degressive combustion). This effect may be the reason for the faster drop in the $\phi_{ex}(z)$ values for higher values of the loading density, for which higher values of pressure are attained.

The effect of crushing may not be the only reason for the faster drop in the burning surface for larger Δ values. The conditions of the ignition inside the perforation do not facilitate the process of ignition. Gases penetrating the perforation are cooled faster than gases at the outer surface of the grains. For fine grains, the divergence of the heat flux in the vicinity of the perforation is high. This retards the increase in the temperature at the perforation surface. Therefore, the ignition at the inner surface can be retarded in comparison to the outer surface. This means that the grains burn for a time after ignition of the outer surface as cylindrical grains. The decrease in the outer surface area is not compensated by the increase in the inner surface area. With increasing values of Δ, the burning rate of the outer surface is faster because higher values of pressure correspond to the given z. This causes a larger part of the grain to be burned before the ignition at the inner surface. As a consequence, the degressive parts of $\phi_{ex}(z)$ are broader for higher values of Δ.

The effect of retarded ignition at the inner surfaces of perforated grains causes the burning surface to be lower than the global surface area of all grains. This may act in favor of choosing the θ_2 value. Taking into account the various factors discussed above, it is not possible to choose either θ_1 or θ_2 as the preferred value. However, treating them as lower and the upper limits of the θ value seems to be justified.

All discussed factors that may influence the determined values of coefficients θ and β are illustrated in Figure 11.

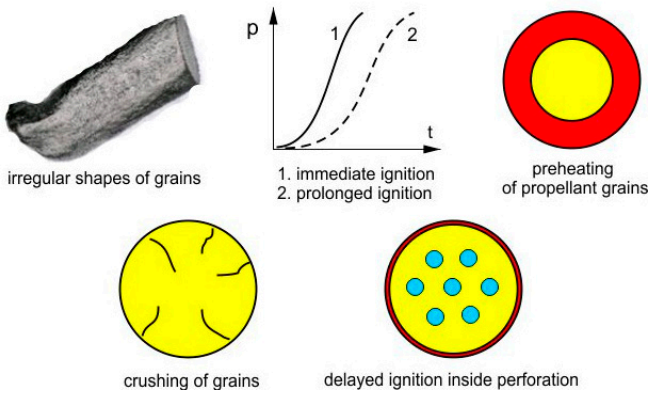

Figure 11. Illustration of factors that may affect determined values of coefficients θ and β.

The described method of determining the α and β values is universal and can be used also for coarse-grained propellants. This aspect enables the method to be validated by comparing the α and β values determined by various methods and by comparison with the literature data for JA-2 propellant (Table 2). The literature data for β values were recalculated using Vielle's equation (Equation (5)). The values denoted as "own 1" were calculated based on the linear approximation of the plots shown in Figure 1. The values

denoted as "own 2" and "own 3" were calculated by the method described in this paper, with β equal to β_1 and β_2, respectively.

Table 2. The values of the exponent α and the coefficient β for JA-2 propellant.

Source	α	β [cm/s]
own 1	0.853	0.0293
own 2	0.842	0.0319
own 3	0.842	0.0323
[20]	0.822	0.0374
[21]	0.847	0.0283
[21]	0.858	0.0265
[21]	0.842	0.0298
[22]	0.952	0.0164
[11]	0.952	0.0163

The values determined for β_1 and β_2 are very close to each other. This is a consequence of the proximity of the experimental form–function plots to the theoretical form–function plot shown in Figure 12. The dependence of the burning rate on the pressure value, calculated based on the α and β values from Table 2, is represented by the plots shown in Figure 13. The burning rate values calculated by the own data used are very close to each other. They are represented by only one plot (dotted line). It is situated in an area limited by the plots based on the literature data. The scatter of the literature data may be a consequence of differences in the characteristics of JA-2 produced by various producers. As stated in the report [23], the burning rates of JA-2 produced in Germany and in the US may differ by 20%.

LO5460 propellant is a good example of coarse-grained propellants with regular shapes of grains. Therefore, it would be desirable to confront the described method with the results obtained in the literature for propellants with irregular shapes of grains. Unfortunately, we did not find any such results. The only exception is the study by [15], in which the results for black powder were analyzed. The shapes of its grains are shown in Figure 14. Shapes are scattered, and it is difficult to classify them. Based on the results of CVT, the value of the exponent α was determined as equal to 0.21. As shown in [15], this value is very close to the value of 0.209, which was deduced in [15], after the analysis of the collection of the literature data concerning the burning rate determined by the strand burner method and published in [24]. Therefore, the method of determining the α value can be assessed as validated for a very demanding case. The value of β is difficult to determine because the theoretical shape function is, in this case, not available. We attempted to assess this value by assuming that the grains shown in Figure 14 have shapes intermediate between the rectangular prism, $1 \times 1 \times 0.5$ mm, and the regular triangle prism of the same thickness and a 1 mm long side. The following values of β_2 were obtained: 1.69 cm/s and 1.15 cm/s. The value of β deduced in [15], based on the plot shown in [24], was equal to 1.2 cm/s, and it is of the same order of magnitude. Plots of the $G(z)$ function obtained in [15] and shown in Figure 15 indicate that the process of the ignition was prolonged. Therefore, the application of the method described in this paper was fully justified.

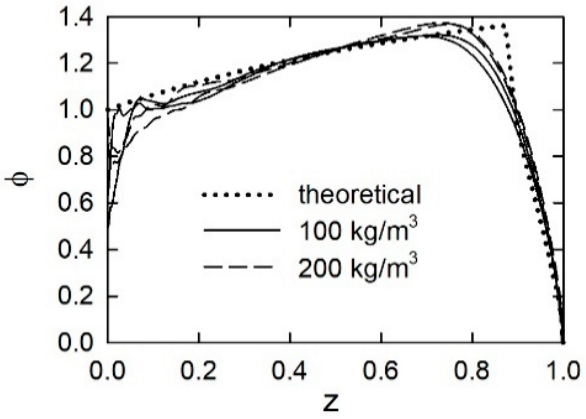

Figure 12. Experimental and theoretical form–function plots for LO5460 (JA-2) propellant.

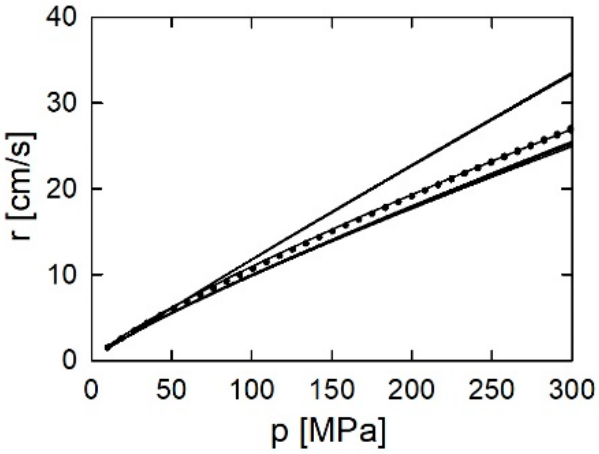

Figure 13. Burning rate dependence on pressure for JA-2 propellant (data from Table 2).

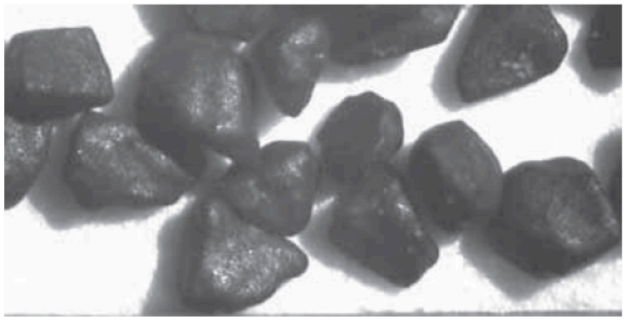

Figure 14. Image of black powder grains [15].

The 12/7 propellant has the same chemical composition as the 5/7NA propellant. However, it can be classified as a coarse-grained propellant. Its S_{g0}/V_{g0} value is only 1.46 times higher than this value for the LO5460 propellant. Figure 15 presents a comparison of the $r(p)$ plots obtained for 5/7NA and 12/7 propellants (β_1 values were chosen). The plots are very close. Thus, the method gives close results for propellants of the same chemical composition, irrespective of the web size. The two propellants have a similar composition to the US M10 propellant. In another report [25], the results of strand burner tests were presented for this propellant. Figure 16 presents the results of those tests. There is a relatively large difference in the burning rate values between 5/7NA and 12/7 propellants and the M10 propellant. This difference can be explained by the difference in the characteristics of the main ingredient of the three propellants—namely, nitrocellulose.

Similar to the case of the JA-2 propellant, nominally, the same composition does not mean the same burning rate values.

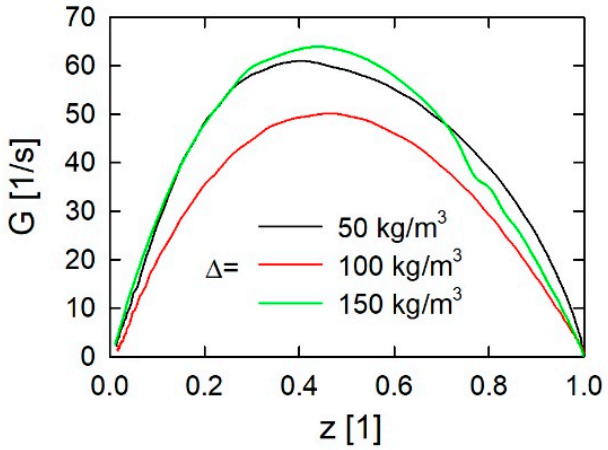

Figure 15. $G(z)$ plots obtained for black powder (recalculated from [15]).

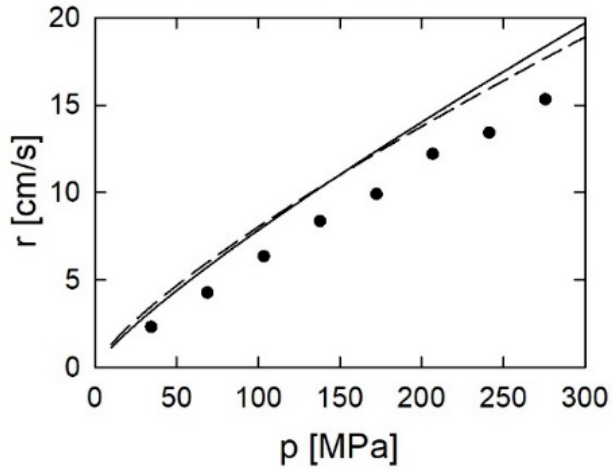

Figure 16. Comparison of the burning rate values obtained for the 5/7NA propellant (solid line) and the 12/7 propellant (dashed line), and strand burner test results for the M10 propellant (circles) [25].

4. Conclusions

1. The prolonged ignition process of fine-grained propellants in CVT is the main source of the difficulties in determining the burning rate. This process runs differently for the different values of the loading density, which complicates the analysis of CVT data.
2. The proposed method assesses the values of the exponent and the coefficient in the burning law with limited accuracy. Nevertheless, its application in the case of coarse-grained propellants provides results agreeing with the standard method.
3. The method provides repeatable results. Thus, a limited number of test repetitions is sufficient to determine the α and β values. In particular, only two values of the loading density are sufficient.

Author Contributions: Conceptualization, R.T.; methodology, Z.L. and R.T.; software, R.T.; validation, Z.L. and Z.S.; formal analysis, Z.L. and R.T.; investigation, Z.L. and Z.S., resources, Z.L. and Z.S.; data curation, R.T.; writing—original draft preparation, R.T.; writing—review and editing, Z.L. and Z.S.; visualization, R.T. and Z.S.; supervision, Z.L.; project administration, Z.L.; funding acquisition, R.T. All authors have read and agreed to the published version of the manuscript.

Funding: This research was funded by the Ministry of Defense of Poland, Grant Number GBMON/13-988/2018/WAT.

Institutional Review Board Statement: Not applicable.

Informed Consent Statement: Not applicable.

Conflicts of Interest: The authors declare no conflict of interest.

References

1. Corner, J. *Theory of the Interior Ballistics of Guns*; John Wiley: New York, NY, USA, 1950.
2. Serebrakov, M. *Interior Ballistics*; Wydawnictwo MON: Warszawa, Poland, 1955. (In Polish)
3. Baer, P.G. *Practical Interior Ballistic Analysis of Guns*; Progress in Astronautics and Aeronautics, Interior Ballistics of Guns; American Institute of Aeronautics and Astronautics: Washington, DC, USA, 1979; Volume 66, pp. 37–66.
4. Carlucci, D.E.; Jacobson, S.S. Ballistics. In *Theory and Design of Guns and Ammunition*; CRC Press: Boca Raton, FL, USA, 2008.
5. *STANAG 4115*; Definition and Determination of Ballistic Properties of Gun Propellants, 2nd ed. Military Agency for Standardization: Brussels, Belgium, 1997.
6. Price, C.; Juhasz, A.A. *Versatile User-Oriented Closed Bomb Data Reduction Program(CBRED)*; BRL-R-2018; US Army Ballistic Research Laboratory: Aberdeen Proving Ground, MD, USA, 1977.
7. Oberle, W.F.; Juhasz, A.; Griffie, T. *A Simplified Computer Code for Reduction to Burning Rates of Closed Bomb Pressure-Time Data (MINICB)*; Report BRL-TR-2841; U.S. Army Research Laboratory: Aberdeen Proving Ground, MD, USA, 1987.
8. Oberle, W.F.; Kooker, D.E. *BRLCB: A Closed-Chamber Data Analysis Program Part I–Theory and User's Manual*; Report ARL-TR-36; US Army Research Laboratory: Aberdeen Proving Ground, MD, USA, 1993.
9. Homan, B.; Juhasz, E. *XLCB: A New Closed-Bomb Data Acquisition and Reduction Program*; Report ARL-TR-2491; US Army Research Laboratory: Aberdeen Proving Ground, MD, USA, 2001.
10. Pocock, M.D.; Guyote, C.C. An Alternative Method for the Derivation of Propellant Burn Rate Data from Closed Vessel Tests. In Proceedings of the 18th International Symposium on Ballistics, San Antonio, TX, USA, 15–19 November 1999; pp. 270–276.
11. Wurster, S. Solid Propellant Burn Rate Measurement in a Closed Bomb. In Proceedings of the 30th International Symposium on Ballistics, Long Beach, CA, USA, 11–15 September 2017; pp. 485–495.
12. Zeldovich, Y.B. On the theory of combustion of propellants and explosives (in Russian). *Zh. Eksp. Teor. Fiz.* **1942**, *12*, 498.
13. Beckstead, M.W.; Puduppakkam, K.; Thakreb, P.; Yang, V. Modeling of Combustion and Ignition of Solid-propellant Ingredients. *Prog. Energy Combust. Sci.* **2007**, *33*, 497–551. [CrossRef]
14. Leciejewski, Z. Singularities of Burning Rate Determination of Fine-Grained Propellants. In Proceedings of the 23rd International Symposium on Ballistics, Tarragona, Spain, 16–20 April 2007; Volume 1, pp. 369–376.
15. Trebinski, R.; Leciejewski, Z.; Surma, Z. Investigations of the Influence of Ignition on the Dynamic Vivacity of Propellants. *Probl. Mechatron. Armament Aviat. Saf. Eng.* **2019**, *10*, 55–68.
16. Trebinski, R.; Leciejewski, Z.; Surma, Z.; Fikus, B. Some Considerations on the Methods of Analysis of Closed Vessel Test Data. In Proceedings of the 29th International Symposium on Ballistics, Edinburgh, UK, 9–13 May 2016; Volume 1, pp. 607–617.
17. Trebinski, R.; Leciejewski, Z.; Surma, Z. Modifications of the closed vessel test results analysis method. In Proceedings of the 31st International Symposium on Ballistics, Hyderabad, India, 4–7 November 2019.
18. Lengellé, G.; Duterque, J.; Trubert, J.F. *Combustion of Solid Propellants*; Report RTO-EN-023; STO Educational Notes: Brussels, Belgium, 2004.
19. Trebinski, R.; Janiszewski, J.; Leciejewski, Z.; Surma, Z.; Kaminska, K. On Influence of Mechanical Properties of Gun Propellants on Their Ballistic Characteristics Determined in Closed Vessel Tests. *Materials* **2020**, *13*, 3243. [CrossRef] [PubMed]
20. Kuo, K.K.; Zhang, B. Transient Burning Characteristics of JA2 Propellant Using Experimentally Determined Zel'dovich Map. *J. Propuls. Power* **2006**, *22*, 455–461. [CrossRef]
21. Manning, G.T.; Leone, J.; Zebregs, M.; Ramlal, R.D.; van Driel, A.C. Definition of a JA-2 Equivalent propellant to be produced by Continuous Solventless Extrusion. *J. Appl. Mech.* **2013**, *80*, 031405. [CrossRef]
22. Juhasz, A.; Bullock, C.; Homan, B.E.; Devynck, D. Micro Closed Bomb for Characterizing the Burning of Propellants at Gun Pressures. In Proceedings of the 36th JANNAF Combustion Subcommittee Meeting, Cocoa Beach, FL, USA, 18–21 October 1999; Volume 692.
23. Miller, M.S.; Anderson, W.R. *CYCLOPS, a Breakthrough Code to Predict Solid-Propellant Burning Rates*; ARL-TR-2910; US Army Research Laboratory: Aberdeen Proving Ground, MD, USA, 2003.
24. Williams, F.A. Observations on Burning and Flame-Spread of Black Powder. *AIAA J.* **1976**, *14*, 637–645. [CrossRef]
25. Grollman, B.B.; Nelson, C.W. *Burning Rates of Standard Army Propellants in Strand Burner and Closed Vessel Tests*; BRL Memorandum Report 2775; US Ballistic Research Laboratory: Aberdeen Proving Ground, MD, USA, 1977.